

# The Interface Chemistry between Chalcogenide Clusters and Open Framework Chalcogenides

PINGYUN FENG,<sup>\*,‡</sup> XIANHUI BU,<sup>†</sup> AND NANFENG ZHENG<sup>‡</sup>

*Department of Chemistry, University of California, Riverside, California 92521, and Department of Chemistry and Biochemistry, California State University, Long Beach, 1250 Bellflower Boulevard, Long Beach, California 90840*

Received July 8, 2004

## ABSTRACT

One of the most exciting recent developments concerning molecular architectures is the emerging field of crystalline chalcogenide superlattices that bridges two traditional but distinct areas of research: chalcogenide clusters and porous materials. By combining synthetic and structural concepts in these two areas, many crystalline solids containing spatially organized chalcogenide clusters have been created that exhibit varied properties ranging from microporosity, fast ion conductivity, and photoluminescence to narrow and tunable electronic band gaps. The potential applications of these materials extend beyond traditional areas such as acid catalysis or adsorption-based separation to include shape- or size-selective photocatalysis, solid-state ionics, and electrochemistry.

## Introduction

The recent development of crystalline porous materials based on chalcogenides has blended two different areas of research: chalcogenide molecular clusters and extended framework solids. The impact of the integration between cluster chemistry and porous solids is being felt in both areas as evidenced by the synthesis of new chalcogenide clusters and open framework solids.<sup>1,2</sup>

The study of chalcogenide superlattices provides a valuable opportunity to explore the synthetic and structural chemistry at the interface of chalcogenide molecular chemistry and solid-state chemistry. This area of research

has become increasingly important because of its relevance to a wide range of fundamental sciences and technological applications. On one hand, molecular chalcogenide clusters represent the lower limit of nanoparticles of which the unique size-dependent properties have been recognized as key to future technological advancement.<sup>3,4</sup> Chalcogenide clusters, being well defined in size and composition, could provide synthetic and structural insights that may help the synthetic design of colloidal nanostructures. On the other hand, applications of crystalline porous solids have been hindered by lack of electronic, optical, or electrooptic properties. Porous materials derived from the organization of chalcogenide clusters could serve as a unique type of materials that integrate uniform porosity with classical semiconductor-type solid-state properties. Such materials may form the basis for a new generation of solid-state devices.

## From Microporous Oxides to Chalcogenides

The interest in crystalline porous materials began with oxides because of the natural occurrence of mineral zeolites. Synthetic zeolites developed since the late 1940s are among the most important microporous materials for industrial applications.<sup>5</sup> Over the past several decades, there has been an increasing interest in the synthesis of new porous materials.<sup>6,7</sup> A major expansion occurred in 1982 when a family of molecular sieves based on aluminophosphates were reported.<sup>5,6</sup>

The explosive growth in the number of microporous and open framework materials is largely due to many variable synthetic and structural parameters. Among these, the use of structure-directing agents with different charge, size, and shape is particularly effective in assisting the formation of oxide frameworks.<sup>8</sup> Furthermore, the systematic and controlled variation of framework cations has led to a variety of open framework solids.<sup>6</sup>

Since late 1980s and the early 1990s, researchers began to explore other framework compositions based on the replacement of O<sup>2-</sup> with other anionic (or neutral) species.<sup>9–11</sup> One method makes use of organic ligands to join together cationic species such as individual metal cations and metal–oxygen clusters.<sup>7</sup> Another method, which is a topic in this Account, sought to create chalcogenide zeolite analogues.<sup>9–12</sup>

Prior to the development of open framework chalcogenides, tetrahedral clusters were not commonly encountered among open framework solids. Microporous oxides such as zeolites are viewed as built from secondary building units that are small rings such as 4-rings (four tetrahedral cations, oxygen not counted) and small cages such as double 4-rings. In open framework chalcogenides, however, a higher structural hierarchy often exists. Superimposed over the above structural features are chalcogenide clusters that behave like large artificial atoms. To construct open framework topology, chalcogenide

Pingyun Feng received her Ph.D. from the Department of Chemistry, University of California at Santa Barbara (1998), with Professor Galen Stucky. From 1998 to 2000, she did her postdoctoral work with Professor David Pine at the Department of Chemical Engineering, University of California at Santa Barbara. She joined the faculty at University of California at Riverside in 2000 and became an associate professor in 2004. She is a recipient of the Alfred P. Sloan research fellowship, Beckman Young Investigator award, Camille Dreyfus Teacher–Scholar Award, and NSF career award.

Xianhui Bu received his Ph.D. from the Department of Chemistry, State University of New York at Buffalo (1992), with Professor Philip Coppens. Between 1992 and 2003, he did his research work with Prof. Galen Stucky at the Department of Chemistry, University of California at Santa Barbara, while supervising the X-ray diffraction facility for the College of Letters and Science. He joined the faculty at California State University, Long Beach, in 2003.

Nanfeng Zheng received his B.S. (1998) in chemistry from Xiamen University, China. He is currently a doctoral candidate at the Department of Chemistry, University of California at Riverside. In 2004, he received a Silver Graduate Student Award from the Materials Research Society.

<sup>‡</sup> University of California, Riverside.

<sup>†</sup> California State University, Long Beach.

**Table 1. A Summary of Supertetrahedral Clusters**

$n$	stoichiometry of $T_n$	examples
1	$MX_4$	$MS_4^{6-}$ ( $M = Mn, Fe, Cd$ )
2	$M_4X_{10}$	$Ge_4E_{10}^{4-}$ ( $E = S, Se$ ), <sup>29,33</sup> $Sn_4E_{10}^{4-}$ ( $E = Se, Te$ ), <sup>34</sup> $M_4S_{10}^{8-}$ ( $Ga, In$ ), $In_4Se_{10}^{8-}$ , <sup>35</sup> $[M_4(SPh)_{10}]^{2-}$ ( $M = Fe, Co, Cd$ ) <sup>4</sup>
3	$M_{10}X_{20}$	$M_{10}S_{20}^{10-}$ ( $M = In, Ga$ ), <sup>14,28</sup> $[M_{10}E_4(SPh)_{16}]^{4-}$ ( $M = Zn, Cd$ ; $E = S, Se$ ; Ph is a phenyl group) <sup>4</sup>
4	$M_{20}X_{35}$	$M_4In_{16}S_{35}^{14-}$ ( $M = Mn, Fe, Co, Zn, Cd$ ) <sup>15,25</sup>
5	$M_{35}X_{56}$	$[Cu_5In_{30}S_{56}]^{17-}$ , <sup>16</sup> $[Zn_{13}In_{22}S_{56}]^{20-}$ <sup>17</sup>
6	$M_{56}X_{84}$	none
$\geq 7$	$M_xX_y^a$	none

$$^a x = [n(n+1)(n+2)]/6; y = [(n+1)(n+2)(n+3)]/6.$$

clusters with divergent coordination geometry is preferable. Therefore, tetrahedrally shaped clusters capable of forming linkages through their corners are of particular interest. In this case, the tetrahedral cluster behaves like a pseudo-tetrahedral atom.<sup>14</sup>

One important reason for the difference between open framework chalcogenides and oxides is the large size of the sulfur atom. The coordination number of sulfur can easily go up to 4 even with relatively large metal cations such as  $Cd^{2+}$  and  $In^{3+}$ . In comparison, tetrahedrally coordinated oxygen sites are rather uncommon in open framework solids due to the small size of the oxygen atom.<sup>13</sup> As a result, open framework chalcogenides represent a rather unique system in which both framework cations and anions have a tendency to form tetrahedral

coordination, in contrast with zeolites or zeolite-like oxides in which only metal cations tend to adopt tetrahedral coordination and the framework oxygen atoms are usually bi- or tricoordinated. While zeolite structures can be described as a net of tetrahedral atoms, cluster-based chalcogenide frameworks can usually be described as a net of clusters with an additional level of structural variations within each individual cluster.<sup>14</sup> Thus open framework chalcogenides can be tuned at two different length scales, providing an additional opportunity to control their properties.

## Chemical and Mathematical Series of Tetrahedral Clusters

The simplest tetrahedral clusters are called supertetrahedral clusters denoted  $T_n$  (Table 1, Figure 1).<sup>14</sup> These are regular tetrahedrally shaped fragments of the cubic ZnS-type lattice. As shown in Table 1, the number of anions in a  $T_n$  cluster is equal to the number of cations in a  $T(n+1)$  cluster. Here,  $n$  is the number of metal layers in each cluster. The number of cations (or anions) within each layer follows a simple series: 1, 3, 6, ...,  $n(n+1)/2$ .

If all metal sites are occupied by  $M^{2+}$  ions, anions on edges and at corners will be underbonded to framework metal cations. The total number of these sites in a  $T_n$  cluster is  $6(n-1) + 4$ . Anions at these sites usually exist as thiolate. For example, the stoichiometry for the  $T_3$  cluster would be  $M_{10}X_4(XR)_{16}$ , where R is an organic group and X is a chalcogen such as S or Se.<sup>4</sup> Alternatively, the

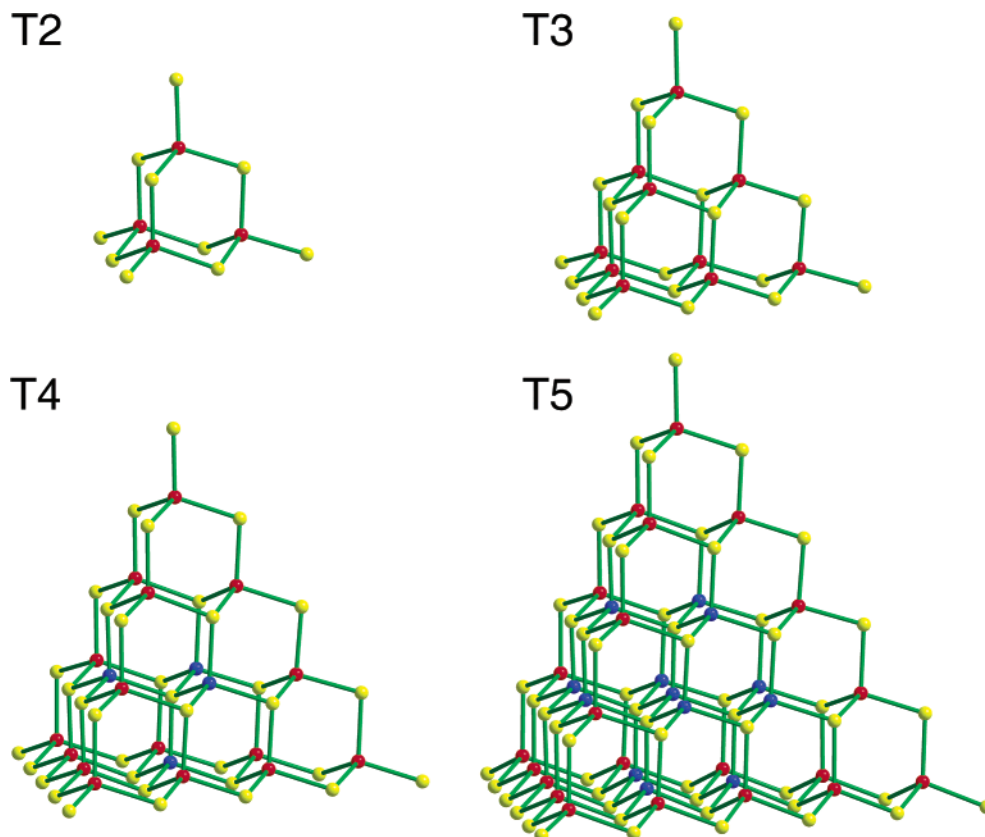


**FIGURE 1.** Ball-and-stick diagrams of  $T_2$ ,  $T_3$ ,  $T_4$ , and  $T_5$  supertetrahedral clusters. Cations and anions sites are shown as red and yellow, respectively. In clusters with both  $M^{2+}$  and  $M^{3+}$  cations, blue sites are generally occupied with  $M^{2+}$  cations.

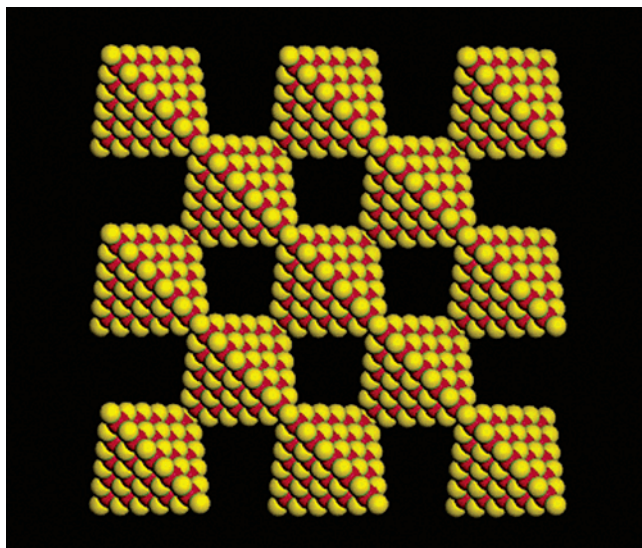


**FIGURE 2.** The top view of the two-dimensional sheet structure built from corner-sharing T5 supertetrahedral clusters ( $\text{Cu}_5\text{In}_{30}\text{S}_{54}^{13-}$ ) in UCR-16.

**Table 2. A Summary of Penta-supertetrahedral Clusters**

$n$	stoichiometry of $P_n$	examples
1	$\text{M}_8\text{X}_{17}$	$\text{M}_4\text{Sn}_4\text{S}_{17}^{10-}$ ( $\text{M} = \text{Mn, Fe, Co, Zn}$ ), <sup>36</sup> $\text{M}_4\text{Sn}_4\text{Se}_{17}^{10-}$ ( $\text{M} = \text{Mn, Zn, Co}$ ) <sup>37,38</sup>
2	$\text{M}_{26}\text{X}_{44}$	$\text{Li}_4\text{In}_{22}\text{S}_{44}^{18-}$ , <sup>2</sup> $\text{Cu}_{11}\text{In}_{15}\text{Se}_{16}(\text{SePh})_{24}(\text{PPh}_3)_4$ <sup>39</sup>
3	$\text{M}_{60}\text{X}_{90}$	none
$\geq 4$	$\text{M}_x\text{X}_y^a$	none

<sup>a</sup>  $x = [4n(n+1)(n+2)]/6 + [(n+1)(n+2)(n+3)]/6$ ;  $y = [4(n+1)(n+2)(n+3)]/6 + [n(n+1)(n+2)]/6$ .

underbonding of sulfur sites could be alleviated if edge and corner  $\text{M}^{2+}$  ions are replaced with  $\text{M}^{3+}$  ions.<sup>15</sup>

The stoichiometry shown above is for isolated clusters. For a network of covalently connected clusters, the overall stoichiometry of the framework varies depending on the pattern of connectivity. One common situation is corner sharing of all four corners of each cluster. This will reduce the total number of anions by 2.

The coordination number of anions is an important concern in the synthetic design of supertetrahedral clusters. While a T2 cluster consists of only bicoordinated anions, the face center of a T3 cluster is occupied by a tricoordinated anion. T1, T2, and T3 clusters have no core atom, whereas the core atom in a T4 cluster is a sulfur atom that can be considered as T0. For even larger clusters, the core atoms form a  $T(n-4)$  cluster. All core ions are tetrahedrally coordinated. The T5 cluster is so far the largest known supertetrahedral cluster and occurs in covalent 3D or 2D superlattices (Figure 2).<sup>16,17</sup> Isolated supertetrahedral clusters with size up to T3 are known.<sup>4</sup>

Another series of tetrahedral clusters are called penta-supertetrahedral clusters denoted as  $P_n$ . The general stoichiometry can be derived if each  $P_n$  cluster is treated as an assemblage of four  $T_n$  clusters tetrahedrally distributed onto four faces of one anti- $T_n$  cluster (Table 2, Figure 3). Here, an anti- $T_n$  cluster is defined as a  $T_n$  cluster with interconverted cationic and anionic sites.

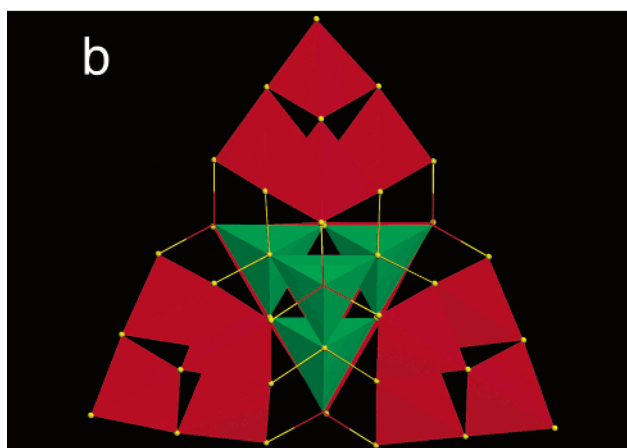
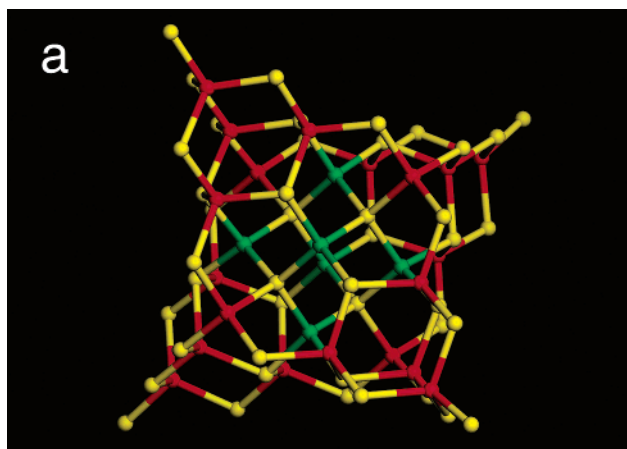


**FIGURE 3.** Two different views of the P2 cluster in ICF-26,  $\text{Ca}_{1.5}\text{Li}_{11}(\text{In}_{22}\text{Li}_4\text{S}_{42})\cdot 44\text{H}_2\text{O}$ : (a) the ball-and-stick view of the P2 cluster,  $\text{Li}_4\text{In}_{22}\text{S}_{44}^{18-}$  in which red denotes  $\text{In}^{3+}$ , green denotes mixed  $\text{In}^{3+}/\text{Li}^+$  sites, and yellow denotes  $\text{S}^{2-}$ ; (b) four supertetrahedral T2 clusters (red) covalently bonded to one anti-supertetrahedral T2 cluster (green) to form a P2 cluster.

The first member (i.e.,  $[\text{S}_4\text{Cd}_{17}(\text{SPh})_{28}]^{2-}$ ) of the third series of tetrahedral clusters was reported in 1988.<sup>18</sup> Like in  $T_n$  clusters, the number of anions is equal to the number of cations in the next member. Isolated clusters of the first two members have been made.<sup>19</sup> For the first member, the covalent superlattices are also known.<sup>20</sup> The third series of tetrahedral clusters are termed as capped supertetrahedral clusters (denoted as  $C_n$ ) here because each consists of a regular supertetrahedral cluster ( $T_n$ ) at the core covered with a shell of atoms the stoichiometry of which is also related to the  $T_n$  cluster (Table 3). Specifically, each face of the  $T_n$  core unit is covered with a single sheet of atoms called the  $T(n+1)$  sheet and each corner of this cluster is covered with a MX group. The  $T(n+1)$  sheet is defined as the bottom atomic sheet of a  $T(n+1)$  cluster.

Additional series of clusters denoted as  $C_{n,m}$  ( $m = 1-4$ ) could be derived starting from the  $C_n$  series. The  $C_{n,m}$  series of clusters has the same composition as the corresponding  $C_n$  cluster but has a different arrangement of the corner atomic unit. The corner atomic unit is a  $\text{M}_4\text{X}_5$  group shaped like barrelene. The  $C_{n,m}$  cluster can be obtained by rotating the corner  $\text{M}_4\text{X}_5$  group in the  $C_n$

**Table 3. A Summary of Capped Supertetrahedral Clusters**

$n$	stoichiometry of $C_n$	examples
1	$M_{17}X_{32}$	$[S_4Cd_{17}(SPh)_{28}]^{2-}$ , <sup>18</sup> $Cd_{17}S_4(SCH_2CH_2OH)_{26}$ <sup>20</sup>
2	$M_{32}X_{54}$	$[S_4Cd_{17}(SPh)_{24}(CH_3OCS_2)_{4/2}]_n \cdot nCH_3OH$ <sup>40</sup> $Cd_{32}S_{14}(SC_6H_5)_{36} \cdot (DMF)_4$ <sup>19</sup> $Cd_{32}S_{14}(SCH_2CH(OH)CH_3)_{36} \cdot 4H_2O$ <sup>41</sup> $Cd_{32}Se_{14}(SePh)_{36}(PPh_3)_4$ <sup>42</sup>
3	$M_{54}X_{84}$	none
$\geq 4$	$M_xX_y^a$	none

$$^a x = [n(n+1)(n+2)]/6 + [4(n+1)(n+2)]/2 + 4; y = [(n+1)(n+2)(n+3)]/6 + [4(n+2)(n+3)]/2 + 4.$$

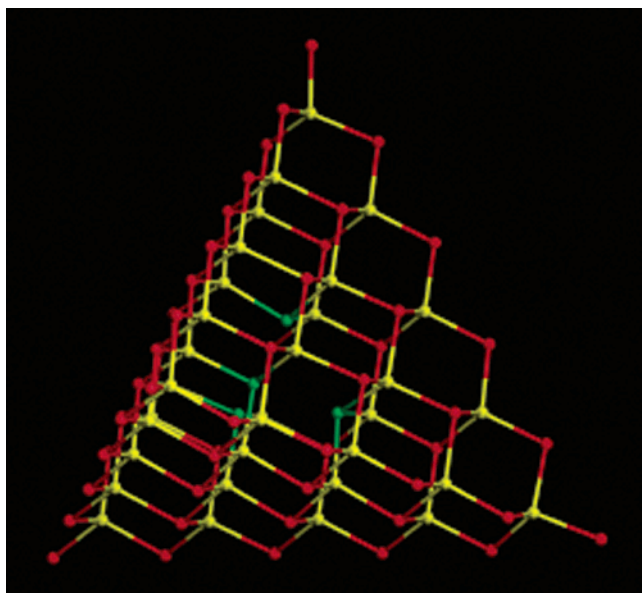


**FIGURE 4.** The structural diagram of the pseudo-T5 cluster ( $In_{34}S_{54}^{6-}$ ) in UCR-15 showing the missing core site surrounded by four core  $S^{2-}$  ions (in green). Yellow denotes  $In^{3+}$ ; red denotes  $S^{2-}$  ions on the surface of the cluster.

cluster by  $60^\circ$ . Each of the four corner units can be independently rotated ( $m$  is the number of corners being rotated), resulting in four series of capped tetrahedral clusters.



**FIGURE 5.** In UCR-15, four T3 clusters ( $In_{10}S_{18}^{6-}$ ) are joined together by a pseudo-T5 cluster ( $In_{34}S_{54}^{6-}$ ) and vice versa.

A multiseried hollow clusters can be generated if each tetrahedral site in a  $Tq$  cluster is replaced with a  $Tp$  cluster. These clusters are called super-supertetrahedral clusters and are denoted as  $Tp,q$ .<sup>21,22</sup> By adding atoms into or removing atoms from regular tetrahedral clusters, other variations of clusters are possible. For example,  $TMA_2Sn_5Se_{10}O$  has a three-dimensional (3D) framework with alternating T1 ( $SnSe_4^{4-}$ ) and stuffed T2 clusters ( $Sn_4S_{10}O^{6-}$ ).<sup>23</sup> Two solids were recently reported that contain the coreless T5 cluster in which the central metal site of the T5 cluster is left empty (Figure 4).<sup>24</sup> In UCR-15, this coreless T5 cluster alternates with a regular T3 cluster to form an interpenetrating diamond-type structure (Figure 5).

#### Factors Affecting the Size of Chalcogenide Clusters.

Metal cations suitable for forming tetrahedral clusters are usually from groups 12–14 (e.g., Zn, Cd, Ga, In, Ge, and Sn) and first-row transition elements such as Mn, Fe, Co, and Cu.<sup>25</sup> Recent synthetic efforts generally involve chalcogenides with only one ( $M^{4+}$ ,  $M^{3+}$ , and  $M^{2+}$ ) or two framework cations ( $M^{4+}/M^{3+}$ ,  $M^{4+}/M^{2+}$ ,  $M^{4+}/M^+$ ,  $M^{3+}/M^{2+}$ , and  $M^{3+}/M^+$ ). There are very few reported open framework chalcogenides with more complex compositions.

The charge on metal cations is an important factor affecting the size of chalcogenide clusters. The effect is related to Pauling's electrostatic valence rule that states that the valence of each anion is exactly or nearly equal to the sum of the electrostatic bond strength to it from adjacent cations. For structures with regular polyhedral geometry, the electrostatic bond strength is often estimated as the ratio of the charge on a cation to its coordination number. A more accurate calculation of the bond valence makes use of each individual bond length and the empirical model proposed by Brown.<sup>26</sup> We use the term *local charge balance* to refer to this situation where the charge of an anion is balanced locally by its adjacent cations. The local charge balance is in contrast with another term called *global charge balance*, which we use to refer to the overall charge density matching between the host framework and the structure-directing agent.

There is a slight difference when the electrostatic valence rule is applied to surface sites and core sites. Anions on the surface of the cluster may receive additional bond valence from positively charged ions that are not part of the cluster. In comparison, the bond valence for core anion sites comes only from those cations that are part of the cluster.

Divalent metal cations have been widely used for preparing chalcogenide clusters. For edge or corner sulfur sites, the coordination number to framework metal cations is low and the valence sum from adjacent  $M^{2+}$  cations is usually inadequate to balance the  $S^{2-}$  anion. Such sites tend to be occupied by thiolate  $-SR$  groups with the  $-R$  group meeting the additional valence requirement of  $S^{2-}$ .

The use of  $M^{3+}$  (e.g.,  $In^{3+}$  and  $Ga^{3+}$ ) or  $M^{4+}$  cations (e.g.,  $Ge^{4+}$  and  $Sn^{4+}$ ) usually provides enough bond valence to balance edge or corner  $S^{2-}$  anions and thus eliminates the need for organic groups. These purely inorganic clusters generally connect with other clusters to form extended structures. One limitation is that clusters containing only  $M^{3+}$  or  $M^{4+}$  cations are usually small (i.e., T2 or T3). Larger clusters are unlikely to form in  $M^{3+}-S$  or  $M^{4+}-S$  compositions because there would be an overabundance of the total bond valence for core sulfur sites. For example, in the  $Ge-S$  system, the largest  $Tn$  cluster is T2. This is because the charge at cation sites is too high for tricoordinated anion sites in clusters larger than T2. However, stuffing the cluster with oxygen anions helps to divert some bond valence away from sulfur anions, which can be adequate to stabilize tricoordinated sulfur sites. As a result, stuffed T3 clusters,  $[Sn_{10}S_{20}O_4]^{8-}$  do exist. For example,  $[Sn_5S_9O_2][HN(CH_3)_3]_2$  contains  $[Sn_{10}S_{20}]$  clusters, in which each adamantane-type cavity accommodates one  $O^{2-}$  ion to give a cluster  $[Sn_{10}S_{20}O_4]^{8-}$ .<sup>8-27</sup> In the binary  $In-S$  or  $Ga-S$  system, the largest  $Tn$  cluster is T3. To form regular clusters larger than T3,  $M^{2+}$  or  $M^+$  cations need to be included in the core of the cluster.

## From Clusters to Open Framework Chalcogenides

The research on open framework chalcogenides was a natural development of the earlier work on porous oxides. The use of organic amines in the synthesis of zeolites has had a dramatic effect on the later development of open framework solids with other compositions.

Research on microporous sulfides started with  $Ge-S$  and  $Sn-S$  systems, also with organic amines as structure-directing agents.<sup>10</sup> Because open framework chalcogenides are generally based on the linkage of clusters, any factor that limits the formation of clusters will likely place a limit on the types of open framework chalcogenides that can be formed. For example, open framework germanium sulfides have not been known to contain regular supertetrahedral clusters larger than T2.

One contribution of open framework chalcogenide chemistry to cluster chemistry is that it provides a route that allows the assembly of individual clusters into a crystal. The formation of a crystalline solid from clusters gives a significant advantage for the elucidation of the

cluster structure and provides insight into possible types of clusters that might exist in solutions from which they crystallize.

The hydrothermal synthesis of open framework chalcogenides seldom starts with molecular clusters as precursors. Instead, simple elemental forms (e.g., sulfur) and inorganic salts are commonly used. Thus, the initial process usually involves redox chemistry and formation of clusters. Clusters of various types and sizes could coexist in a solution. Equilibria between various clusters in solution would shift to favor one or more clusters when crystallization involving these clusters occurs.

One system that demonstrates the selective crystallization of different clusters is the  $Zn-Ga-S$  mixture containing amine molecules. The presence of both  $M^{2+}$  and  $M^{3+}$  ions in a solution allows the formation of both T3 ( $Ga_{10}S_{20}^{10-}$ ) and T4 ( $Zn_4Ga_{16}S_{35}^{14-}$ ) clusters. In our work, by using different amine molecules, one or both of them can be selectively crystallized into a superlattice. Three new phases denoted as UCR-7, UCR-5 and UCR-19 have been made. All three phases have the same intercluster connectivity (i.e., interpenetrating diamond lattice), and they only differ in the size of clusters at each tetrahedral node (Figure 6). UCR-7 is made from T3 clusters only and UCR-5 is made from T4 clusters. UCR-19 is very unusual and consists of alternating T3 and T4 clusters.<sup>28</sup>

**Amine-Directed Open Framework Chalcogenides.** In oxides, oxygen sites of the anionic framework can form strong hydrogen bonding with  $N-H$  groups of protonated amine molecules. Such  $O\cdots H-N$  bonding is an important factor in the directed assembly of oxide frameworks. In comparison, the hydrogen bonding between chalcogenide frameworks and guest molecules (e.g.,  $S\cdots H-N$ ) is much weaker. The coassembly of chalcogenide clusters with guest molecules depends to a large extent on the host-guest electrostatic interaction. This helps to explain that open framework chalcogenides generally have a rather negative framework and few neutral or nearly neutral open framework chalcogenides are known today. To match the highly negative host framework, guest molecules in open framework chalcogenides usually have a high charge density.

The host-guest charge density matching is also called the global charge matching here, in contrast with the local charge matching. Unlike the local charge matching that in general follows the electrostatic valence rule, the global charge matching is only qualitatively understood and is more difficult to manipulate experimentally. However, its role in the self-assembly process is critical as already shown in the synthesis of both microporous and mesoporous oxides.<sup>8</sup> For example, in the synthesis of aluminophosphates containing divalent metal cations ( $M^{2+}$ ), the  $M^{2+}$  to  $Al^{3+}$  ratio allows a rather flexible adjustment of the framework charge density and therefore makes it easier to achieve the global charge matching.<sup>8</sup> In chalcogenide clusters, the ratio between metal cations of different valences is also subject to the limitation of the local charge balance within each cluster and may not be as flexible as that in oxides.

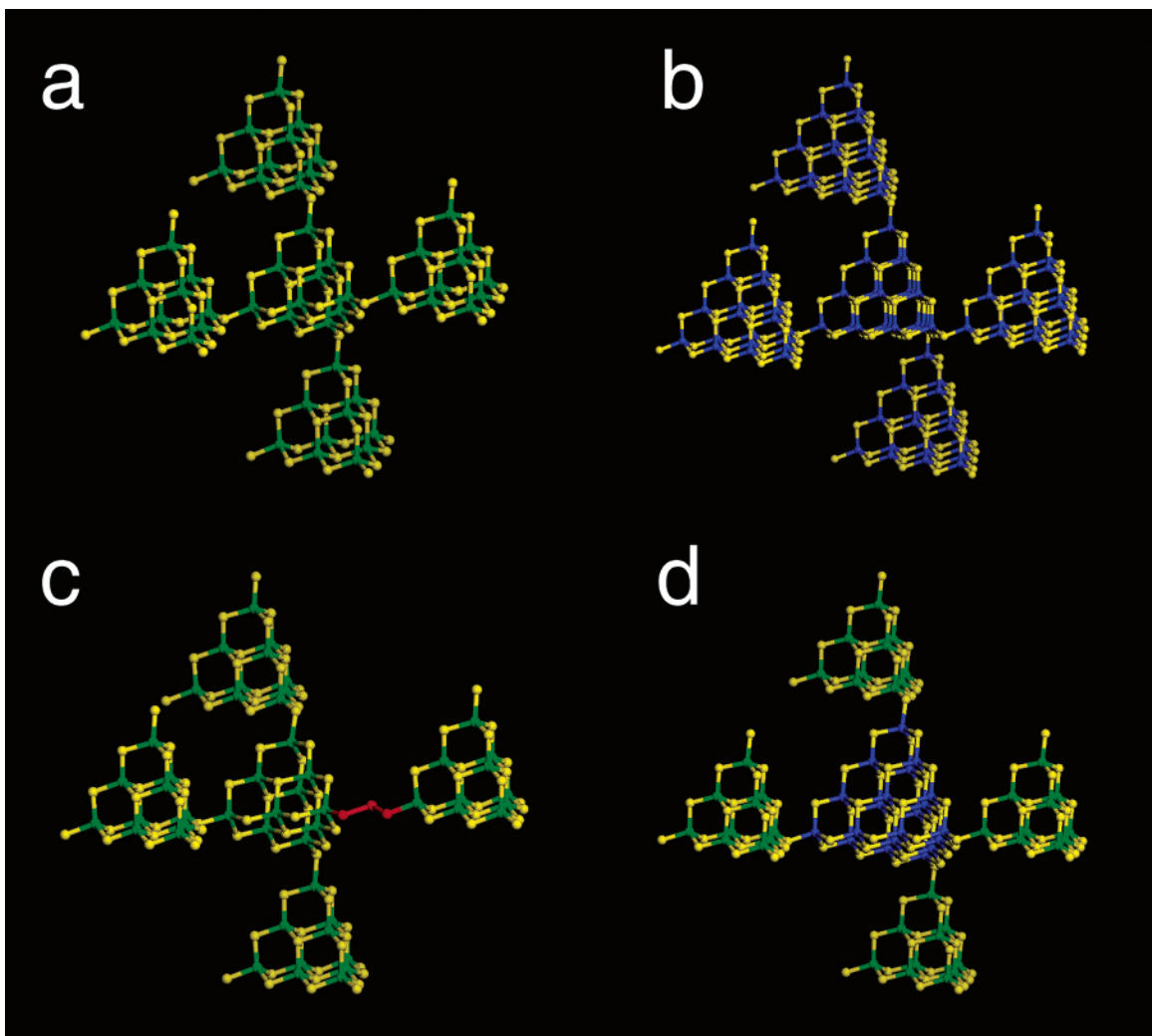


**FIGURE 6.** Four different superlattices made from T3 ( $\text{Ga}_{10}\text{S}_{18}^{6-}$ ) and T4 ( $\text{Zn}_4\text{Ga}_{16}\text{S}_{33}^{10-}$ ) clusters: (a) the T3–T3 superlattice in UCR-7; (b) the T4–T4 superlattice in UCR-5; (c) the T3–T3 superlattice through mixed –S– and –S–S–S– bridges in UCR-18; (d) the hybrid T3–T4 superlattice in UCR-19.

Very few 3D framework structures have been found in Ge–S and Sn–S compositions, even though T2 clusters such as  $\text{Ge}_4\text{S}_{10}^{4-}$  are found to occur frequently. One likely reason is that a fully connected 3D  $\text{M}^{4+}$ –S framework would be neutral and does not allow effective structure directing through host–guest electrostatic interaction.

The inclusion of  $\text{M}^{2+}$  or  $\text{M}^+$  cations into the synthesis mixture of Ge–S and Sn–S systems did help to generate new framework solids.  $\text{M}^{2+}$  or  $\text{M}^+$  cations, when in tetrahedral coordination, create negative centers on the framework that enhance the structure-directing effect of protonated amine molecules. Interestingly, these low-valent cations are not incorporated into the cluster to increase the size of the cluster. Instead, they are found between Ge–S or Sn–S clusters to join these clusters (e.g.,  $\text{Ge}_4\text{S}_{10}^{4-}$ ) into infinite frameworks. One example is the synthesis of a series of compounds with the general formula of  $[(\text{CH}_3)_4\text{N}]_2\text{MGe}_4\text{S}_{10}$  ( $\text{M} = \text{Mn}^{2+}$ ,  $\text{Fe}^{2+}$ , or  $\text{Cd}^{2+}$ ).<sup>29</sup>

A negative framework can also be obtained if tetravalent cations are replaced with trivalent cations. When organic structure-directing agents are used in the  $\text{M}^{3+}$ –S

system, resulting open framework chalcogenides usually contain cross-linked T3 clusters (e.g.,  $\text{In}_{10}\text{S}_{20}^{10-}$ ). Unexpectedly, the effect of adding  $\text{M}^{2+}$  or  $\text{M}^+$  cations into the  $\text{M}^{3+}$ –S system is different from that in the  $\text{M}^{4+}$ –S system. Rather than linking T3 clusters into a network as they did with T2  $\text{Ge}_4\text{S}_{10}^{4-}$  clusters,  $\text{M}^{2+}$  or  $\text{M}^+$  cations can form the central part of new and larger clusters. For example,  $\text{Mn}^{2+}$ ,  $\text{Fe}^{2+}$ ,  $\text{Co}^{2+}$ ,  $\text{Zn}^{2+}$ , and  $\text{Cd}^{2+}$  are all known to form  $\text{M}_4\text{In}_{16}\text{S}_{35}^{14-}$  T4 clusters,<sup>15,25</sup> in which four divalent cations are located on the faces of the cluster to form tetrahedral geometry around the single core sulfur atom.

While the compositional domains described above (i.e.,  $\text{M}^{4+}/\text{M}^{2+}$ ,  $\text{M}^{4+}/\text{M}^+$ ,  $\text{M}^{3+}$ ,  $\text{M}^{3+}/\text{M}^{2+}$ ,  $\text{M}^{3+}/\text{M}^+$ ) do yield a number of interesting open framework chalcogenides, these compositions differ from the composition of zeolites that are built from  $\text{M}^{4+}$  and  $\text{M}^{3+}$  ions. The  $\text{M}^{4+}/\text{M}^{3+}$  was not expected to be simple because either  $\text{M}^{4+}$  or  $\text{M}^{3+}$  could independently form amine-directed crystals with sulfur and thus the probability of phase separation was high. The success with the  $\text{M}^{4+}/\text{M}^{3+}$  system was mainly attributed to the use of the nonaqueous synthesis method discovered earlier with the Ga–S system.<sup>22</sup>

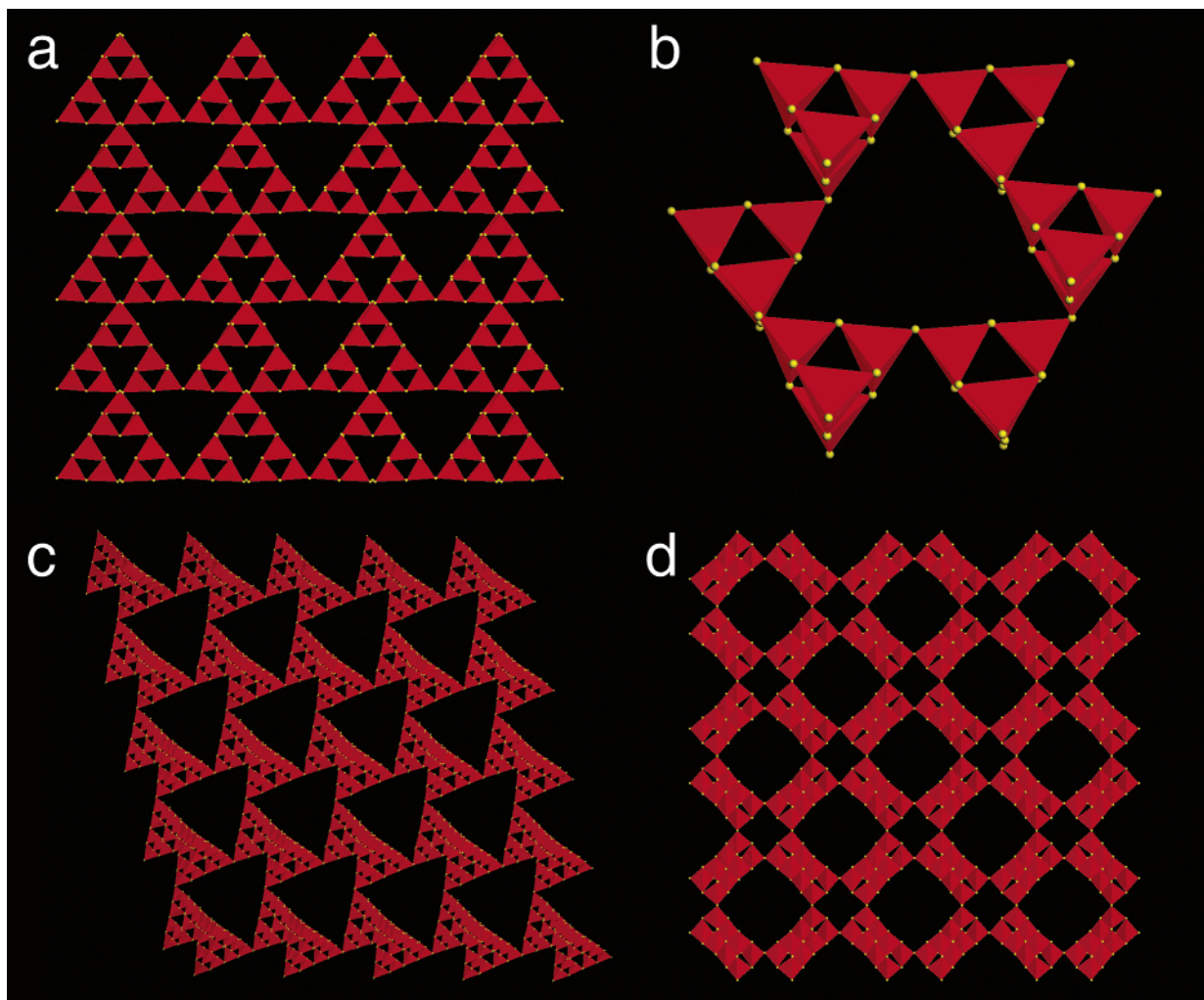


**FIGURE 7.** The four topological types formed in the  $M^{3+}/M^{4+}$  system: (a) the 3D  $M_4X_{10}$  decorated sodalite framework in UCR-20; (b) six  $M_4X_{10}$  clusters joined into a six-membered ring in UCR-21 with the cubic ZnS framework; (c) the 3D framework of UCR-22 with the cubic ZnS type topology decorated with the coreless T4 cluster ( $M_{16}X_{34}$ ) (only one set of lattice in UCR-22 is shown); (d) the 3D framework of UCR-23 with the  $CrB_4$  topology projected down the 16-ring channels. In all structures, the metal site is usually a mixed  $M^{3+}/M^{4+}$  site.

Four different topologies were discovered in the  $M^{4+}/M^{3+}$  system ( $M^{4+} = Ge^{4+}$  or  $Sn^{4+}$ ,  $M^{3+} = Ga^{3+}$  or  $In^{3+}$ ) (Figure 7).<sup>22</sup> While the incorporation of  $M^{2+}$  or  $M^+$  into the  $M^{3+}-S$  system tends to increase the size of the cluster from T3 to T4 or T5, the incorporation of  $M^{4+}$  into the  $M^{3+}-S$  system decreases the size from T3 to T2. Because all anions in the T2 cluster are bicoordinated, which is a key feature of zeolite structures, chalcogenides in the  $M^{4+}/M^{3+}$  system could be described using the same terminology as those for zeolites. Alternatively, each T2 cluster could be treated as a pseudo-tetrahedral atom to obtain a simpler 3D net. In comparison, open framework chalcogenides based on T3 clusters or larger could not be described as 4-connected, 3D nets based on positions of individual framework cations. However, when each T3 or T4 cluster is treated like a pseudo-tetrahedral atom, the resulting net is 4-connected and three-dimensional, just like that in zeolite structures.

**Hydrated Open Framework Chalcogenides.** Crystalline microporous materials began with mineral zeolites in which charge-balancing extraframework cations are hydrated inorganic cations. The past three decades have

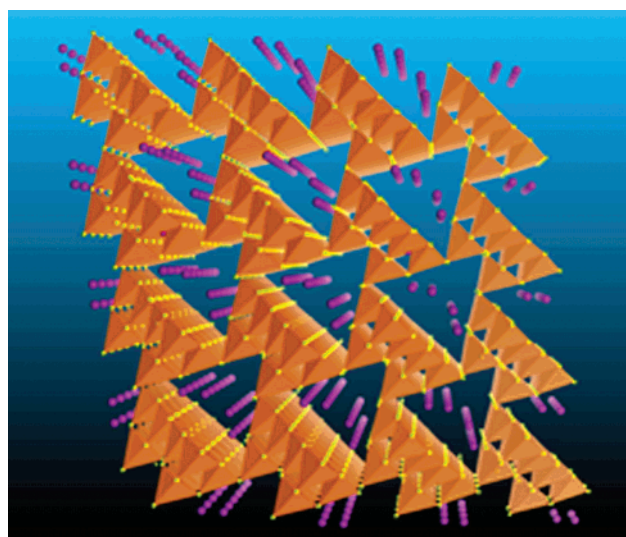


**FIGURE 8.** T2 clusters ( $In_4Se_8^{4-}$ ) in ICF-21InSe—Na are connected into a non-interpenetrating diamond-type lattice. Unconnected spheres are  $Na^+$  sites.

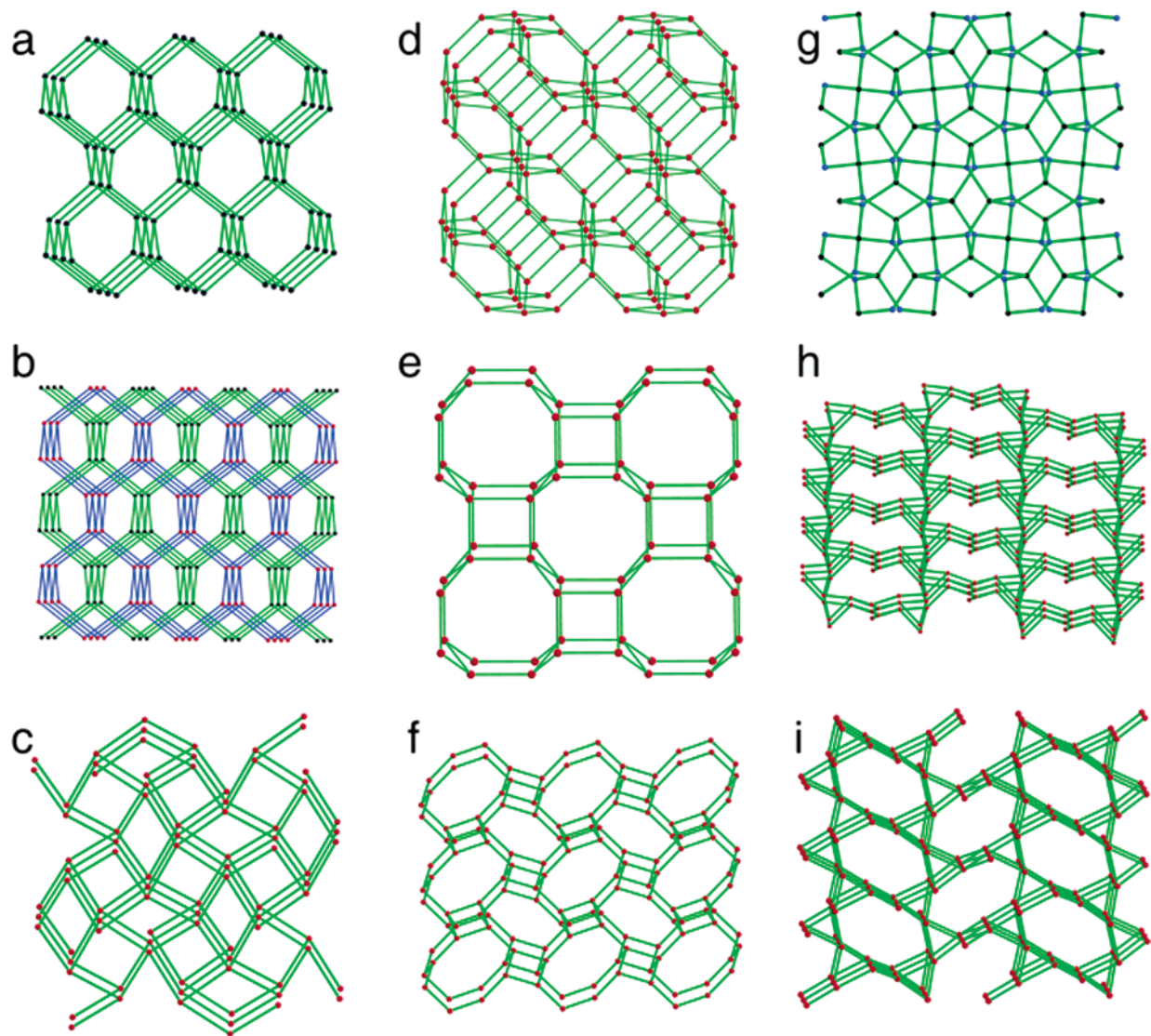


**FIGURE 9.** Examples of 3D framework topologies formed from tetrahedral clusters: (a) single diamond; (b) double diamond; (c) UCR-1; (d) SOD; (e) CrB<sub>4</sub>; (f) ABW; (g) cubic-C<sub>3</sub>N<sub>4</sub>; (h) ICF-24; (i) ICF-25. Except for the cubic-C<sub>3</sub>N<sub>4</sub> type topology, all others are 4-connected 3D nets with each sphere representing a tetrahedral node that can be occupied either by a single tetrahedral atom or in chalcogenides by a tetrahedral cluster. For the cubic-C<sub>3</sub>N<sub>4</sub> type, blue spheres are three-connected sites and black spheres are 4-connected sites.

witnessed a major shift toward the use of organic molecules for the synthesis of porous materials. However, the purely inorganic system continues to exhibit rich synthetic and structural chemistry as demonstrated by the synthesis of a class of hydrated open framework chalcogenides (Figure 8).

Hydrated open framework chalcogenides share structural similarity with amine-directed chalcogenides. Covalent superlattices with T2, T4, and T5 clusters are found in both synthesis systems. So far, hydrated chalcogenides have been made in In<sup>3+</sup>, In<sup>3+</sup>/Cu<sup>+</sup>, In<sup>3+</sup>/M<sup>2+</sup> (M<sup>2+</sup> = Mn, Zn, Cd, ...) compositions.<sup>17</sup> One notable difference is the absence of tetravalent cations in UCR-21 (Na<sub>4</sub>In<sub>4</sub>Se<sub>8</sub>·xH<sub>2</sub>O) and UCR-22 (Li<sub>4</sub>In<sub>4</sub>S<sub>8</sub>·xH<sub>2</sub>O) in the purely inorganic system. In comparison, when amine molecules are used as structure-directing agents, tetravalent cations such as Ge<sup>4+</sup> are included into the same framework to bring down the negative charge. This is apparently an effect of the global charge matching. The exclusion of M<sup>4+</sup>

cations in the hydrated phases results from the high charge density of inorganic cations as compared to organic cations.

So far no T3 clusters have been found in the hydrated system even though four other tetrahedral clusters (i.e., T2, T4, T5, coreless T4) form readily in the hydrated system and T3 clusters are common in the amine-directed system.<sup>17</sup> It is likely that for sulfur sites exposed to highly charged extraframework inorganic cations, the coordination to three additional M<sup>3+</sup> ions becomes unfavorable because of the increased bond valence sum. Thus T3 clusters with S<sup>2-</sup> bonded to three M<sup>3+</sup> ions are not expected to be stable in the inorganic system. This situation does not apply to T4 or T5 clusters because their tricoordinated S sites are bonded to a combination of M<sup>2+</sup> and M<sup>3+</sup> sites.

**Hybrid Inorganic–Organic Open Framework Chalcogenides.** Open framework chalcogenides described above consist of purely inorganic frameworks and inor-



ganic or organic guest species. A new class of open framework chalcogenides can be constructed by using organic multidentate ligands to join together chalcogenide clusters. The feasibility of this synthetic strategy is illustrated by the recent synthesis of an open framework chalcogenide in which cubic  $[\text{Cd}_8(\text{SPh})_{12}]^{4+}$  clusters are linked by a tetradentate ligand, 1,2,4,5-tetra(4-pyridyl)-benzene, into a 3D framework.<sup>30</sup> This material has a positively charged framework, in contrast with other open framework chalcogenides discussed here, all of which have negatively charged frameworks.

## Architectural Features of Open Framework Chalcogenides

Tetrahedral clusters are usually joined together with a single  $\text{S}^{2-}$  (or  $\text{Se}^{2-}$ ) bridge. The consideration of topological features can usually be simplified if we ignore the internal structure of the cluster and consider each cluster as a pseudo-tetrahedral atom. With this simplification, the 3D framework of a chalcogenide can be reduced to that of very simple structure types, two of which (ABW and SOD) are listed as zeolite structure types.

At least nine 3D topological types have been realized from the assembly of tetrahedral clusters (Figure 9). Among these, the single and double diamond type lattices are the most common. For small T2 and T3 clusters, both single and double diamond type structures are known. However, for structures with T3–T4, T4, or larger clusters such as P2 and T5, only the double diamond type has been observed so far. In this case, the lattice interpenetration and guest molecules (or ions) combine to fill the large void space.

Other structure types include ABW,  $\text{CrB}_4$ , SOD, cubic- $\text{C}_3\text{N}_4$ , UCR-1, ICF-24, and ICF-25. The ABW type occurs with T1–T2 clusters.<sup>31</sup> ICF-24 and ICF-25 types have only been made with T2 clusters. The  $\text{CrB}_4$  and sodalite types have been realized with either T2 or T3 clusters. UCR-1 and cubic- $\text{C}_3\text{N}_4$  types only occur with the T4 cluster (Figure 10).<sup>32</sup>

The number of the 3D framework types in open framework chalcogenides remains small now. This is in part due to the inflexibility of the T–S–T angles that are generally within  $10^\circ$  of  $109^\circ$ . The framework topological type is to a large extent determined by the T–X–T angle that can range from about  $100^\circ$  to  $180^\circ$  in open framework oxides. Thus devising new linkage modes among clusters will help to achieve new topological types.

## Selected Properties of Open Framework Chalcogenides

Numerous open framework solids have been made in the past two decades. While these open framework solids possess a wide range of compositions and topological features, their application potential is often limited by their low thermal stability. So far, few open framework chalcogenides are known to show microporosity through gas adsorption. This is because open framework chalcogenides generally have a thermal stability lower than 500

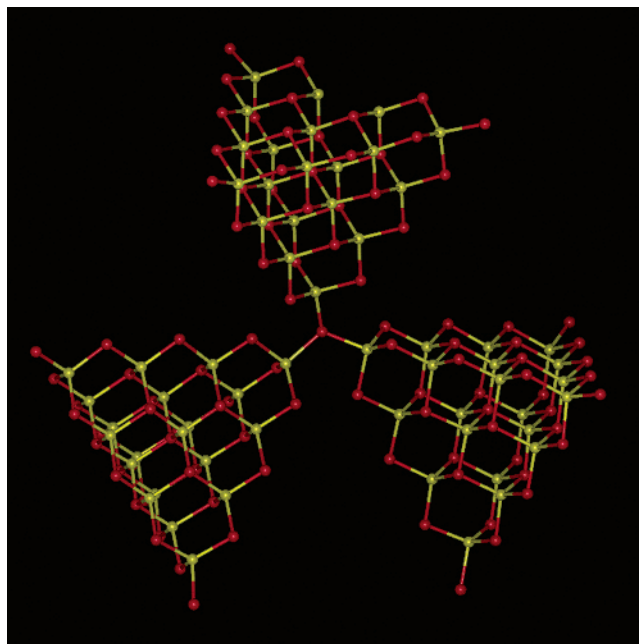


**FIGURE 10.** Three T4 clusters,  $\text{M}_4\text{In}_{16}\text{S}_{35}$  ( $\text{M} = \text{Fe}^{2+}$ ,  $\text{Co}^{2+}$ ,  $\text{Zn}^{2+}$ , and  $\text{Cd}^{2+}$ ), are joined together by sharing a tricoordinated sulfur in UCR-8. Red denotes  $\text{S}^{2-}$ ; yellow denotes  $\text{In}^{3+}$  and  $\text{M}$ .

$^\circ\text{C}$ , which makes it hard to completely remove organic guest molecules through calcination. For example, in one experiment, about 77% of nitrogen and 81% of hydrogen were removed from UCR-20GaGeS-TAEA (TAEA = tris(2-aminoethyl)amine) by direct calcination at  $350^\circ\text{C}$  in nitrogen. However, the coke formation made the removal of carbon difficult. Only about 39% of carbon was removed from UCR-20GaGeS-TAEA in the same experiment.<sup>22</sup>

Ion exchange is among the most common properties of open framework solids. This property has been shown for a number of open framework sulfides, in which protonated amine molecules are exchanged with inorganic cations such as  $\text{Na}^+$ . Microporosity can be produced by removing large organic cations through ion exchange with small inorganic cations. For example, the exchange with  $\text{Cs}^+$  ions led to an almost complete removal of amine molecules from UCR-20GaGeS-TAEA. The  $\text{Cs}^+$ -exchanged UCR-20GaGeS-TAEA exhibits the type I isotherm characteristic of a microporous solid (Figure 11). This sample has a high BET surface area of  $807\text{ m}^2/\text{g}$  and a micropore volume of  $0.23\text{ cm}^3/\text{g}$  despite the presence of much heavier elements (Cs–Ga–Ge–S) compared to those in zeolites.<sup>22</sup>

The electrical conductivity of chalcogenides may consist of contributions from both electronic and ionic conductions. The open framework construction tends to lower the electronic conductivity while promoting the ionic contribution. The direct synthesis of 3D chalcogenides containing mobile alkali metal cations has led to a new class of fast ion conductors.<sup>17</sup> These crystalline inorganic chalcogenides integrate zeolite-like architecture with high anionic framework polarizability and high concentrations of mobile cations. These structural features are particularly desirable for enhancing ionic conductivity. At room temperature and under relative humidity of 30%

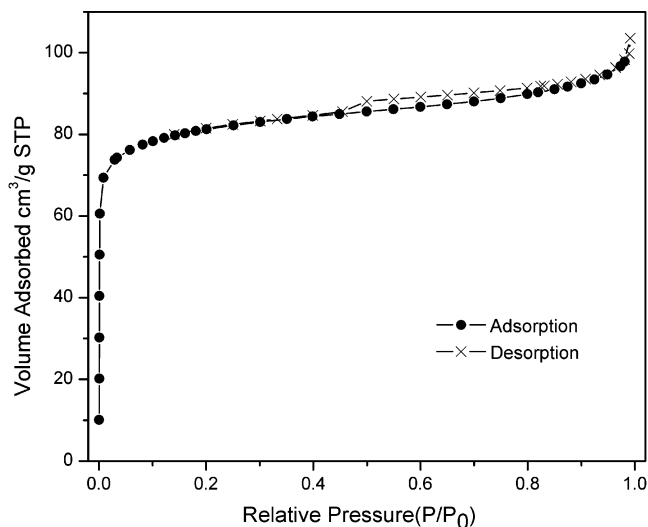


**FIGURE 11.** Nitrogen adsorption and desorption isotherms measured at 77 K for the Cs<sup>+</sup>-exchanged UCR-20GaGeS-TAEA. The ion exchange was performed at 373 K for 60 h and then dried at 353 K for 2 h. Prior to the measurement, the sample was degassed at 373 K for 10 h.

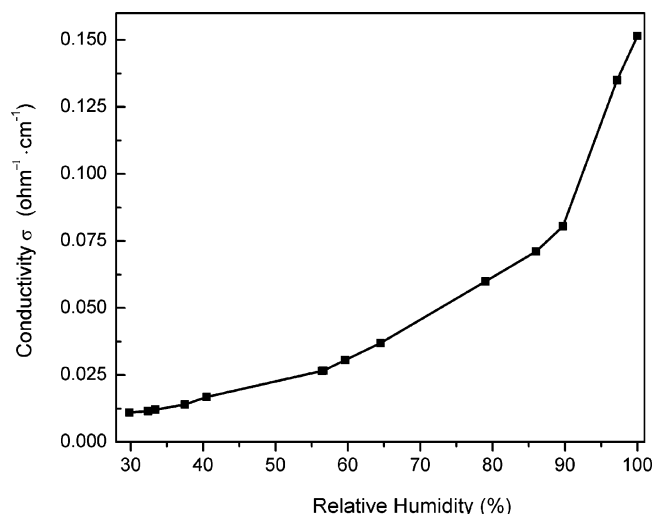


**FIGURE 12.** The ionic conductivity of ICF-26 under different relative humidity. Ionic conductivities were measured on a single crystal (cross section  $0.37 \times 0.43 \text{ mm}^2$ , length 0.63 mm) by ac impedance methods using a Solatron 1260 frequency response analyzer. The resistance decreases from  $3.590 \times 10^3 \Omega$  at 29.8% RH to  $2.614 \times 10^2 \Omega$  at 100% RH.

or higher, the specific conductivity of these materials is comparable to or exceeds previously known crystalline sodium or lithium conductors. In general, the conductivity increases with increasing humidity. The highest specific conductivity achieved among open framework chalcogenides is  $0.15 \Omega^{-1} \text{ cm}^{-1}$  at 27 °C and under 100% relative humidity (Figure 12).<sup>2</sup>

Most open framework chalcogenides have been shown to display photoluminescence with tunable emission wavelengths ranging almost continuously from 450 to 600 nm.<sup>22</sup> The electronic band gaps of these chalcogenides are generally smaller than open framework oxides and many of them are in the visible range. This makes it possible to explore these open framework materials for applications

ranging from solar cells to photocatalysis with visible light. In our preliminary work, some of these open framework chalcogenides have been found to be highly active as visible-light photocatalysts for the reduction of water into hydrogen.

## Conclusions

Impressive synthetic successes have been achieved in the area of porous chalcogenides and chalcogenide clusters, leading to the creation of many new open framework chalcogenides. The synthetic and structural principles developed from these investigations will provide useful guidance for the future exploration of this important area of research. The availability of these interesting materials has made it possible to systematically study various properties and potential applications of these unique materials.

*We acknowledge the support of this work by CSULB (X.B.), the NSF (P.F.), Beckman Foundation (P.F.), and the donors of the Petroleum Research Fund (administered by the ACS) (X.B. and P.F.). P.Y. is an Alfred P. Sloan research fellow and Camille Dreyfus Teacher-Scholar.*

## References

- (1) Bu, X.; Zheng, N.; Feng, P. Tetrahedral Chalcogenide Clusters and Open Frameworks. *Chem.–Eur. J.* **2004**, *10*, 3356–3362.
- (2) Zheng, N.; Bu, X.; Feng, P. Penta-Supertetrahedral Clusters as Building Blocks for Three-Dimensional Sulfide Superlattice. *Angew. Chem., Int. Ed.* **2004**, *43*, 4753–4755.
- (3) Soloviev, V. N.; Eichhofer, A.; Fenske, D.; Banin, U. Size-Dependent Optical Spectroscopy of a Homologous Series of CdSe Cluster Molecules. *J. Am. Chem. Soc.* **2001**, *123*, 2354–2364.
- (4) Dance, I.; Fisher, K. Metal Chalcogenide Cluster Chemistry. In *Progress in Inorganic Chemistry*; Karlin, K. D., Ed.; John Wiley & Sons: New York, 1994; Vol. 41, pp 637–803.
- (5) Flanigen, E. M. Zeolites and Molecular Sieves. An Historical Perspective. In *Introduction to Zeolite Science and Practice*; van Bekkum, H.; Flanigen, E. M.; Jansen, J. C., Eds.; Elsevier: New York, 1991; 13–34.
- (6) Cheetham, A. K.; Ferey, G.; Loiseau, T. Open-framework inorganic materials. *Angew. Chem., Int. Ed.* **1999**, *38*, 3268–3292.
- (7) Yaghi, O. M.; O’Keeffe, M.; Ockwig, N. W.; Chae, H. K.; Eddaoudi, M.; Kim, J. Reticular synthesis and the design of new materials. *Nature* **2003**, *423*, 705–714.
- (8) Feng, P.; Bu, X.; Stucky, G. D. Hydrothermal syntheses and structural characterization of zeolite analogue compounds based on cobalt phosphate. *Nature* **1997**, *388*, 735–741.
- (9) Bows, C. L.; Ozin, G. A. Self-assembling frameworks. Beyond microporous oxides. *Adv. Mater.* **1996**, *8*, 13–28.
- (10) Bedard, R. L.; Wilson, S. T.; Vail, L. D.; Bennett, J. M.; Flanigen, E. M. The next generation: synthesis, characterization, and structure of metal sulfide-based microporous solids. In *Zeolites: Facts, Figures, Future. Proceedings of the 8th International Zeolite Conference*; Jacobs, P. A., van Santen, R. A., Eds.; Elsevier: Amsterdam, 1989; p 375.
- (11) Scott, R. W. J.; MacLachlan, M. J.; Ozin, G. A. Synthesis of metal sulfide materials with controlled architecture. *Curr. Opin. Solid State Mater. Sci.* **1999**, *4*, 113–121.
- (12) Cahill, C. L.; Parise, J. B. On the formation of framework indium sulfides. *J. Chem. Soc., Dalton Trans.* **2000**, 1475–1482.
- (13) There are some exceptions. In particular, the tetrahedral unit, Zn<sub>4</sub>O<sup>6+</sup>, is known in a number of open-framework solids. Li, H.; Eddaoudi, M.; O’Keeffe, M.; Yaghi, M. Design and synthesis of an exceptionally stable and highly porous metal-organic framework. *Nature* **1999**, *402*, 276–279.
- (14) Li, H.; Laine, A.; O’Keeffe, M.; Yaghi, O. M. Supertetrahedral sulfide crystals with giant cavities and channels. *Science* **1999**, *283*, 1145–1147.
- (15) Li, H.; Kim, J.; Groy, T. L.; O’Keeffe, M.; Yaghi, O. M. 20 Å Cd<sub>4</sub>In<sub>16</sub>S<sub>35</sub><sup>14-</sup> Supertetrahedral T4 Clusters as Building Units in Decorated Cristobalite Frameworks. *J. Am. Chem. Soc.* **2001**, *123*, 4867–4868.

- (16) Bu, X.; Zheng, N.; Li, Y.; Feng, P. Pushing Up the Size Limit of Chalcogenide Supertetrahedral Clusters: Two- and Three-Dimensional Photoluminescent Open Frameworks from  $(\text{Cu}_5\text{In}_{30}\text{S}_{54})^{13-}$  Clusters. *J. Am. Chem. Soc.* **2002**, *124*, 12646–12647.
- (17) Zheng, N.; Bu, X.; Feng, P. Synthetic design of crystalline inorganic chalcogenides exhibiting fast-ion conductivity. *Nature* **2003**, *426*, 428–432.
- (18) Lee, G. S. H.; Craig, D. C.; Ma, I.; Scudder, M. L.; Bailey, T. D.; Dance, I. G.  $[\text{S}_4\text{Cd}_{17}(\text{SPh})_{28}]^{2-}$ , the first member of a third series of tetrahedral  $[\text{S}_n\text{M}_x(\text{SR})_y]^{z-}$  clusters. *J. Am. Chem. Soc.* **1988**, *110*, 4863–4864.
- (19) Herron, N.; Calabrese, J. C.; Farneth, W. E.; Wang, Y. Crystal structure and optical properties of  $\text{Cd}_{32}\text{S}_{14}(\text{SC}_6\text{H}_5)_{36}\text{DMF}_4$ , a cluster with a 15 angstrom cadmium sulfide core. *Science* **1993**, *259*, 1426–1428.
- (20) Vossmeier, T.; Reck, G.; Katsikas, L.; Haupt, E. T. K.; Schulz, B.; Weller, H. A Double Diamond Superlattice Built Up of  $\text{Cd}_{17}\text{S}_4(\text{SCH}_2\text{CH}_2\text{OH})_{26}$ . *Science* **1995**, *267*, 1476–1479.
- (21) Li, H.; Kim, J.; O'Keeffe, M.; Yaghi, O. M.  $[\text{Cd}_{16}\text{In}_6\text{S}_{134}]^{44-}$ : 31-Å tetrahedron with a large cavity. *Angew. Chem., Int. Ed.* **2003**, *42*, 1819–1821.
- (22) Zheng, N.; Bu, X.; Wang, B.; Feng, P. Microporous and Photoluminescent Chalcogenide Zeolite Analogues. *Science* **2002**, *298*, 2366–2369.
- (23) Ahari, H.; Lough, A.; Petrov, S.; Ozin, G. A.; Bedard, R. L. Modular assembly and phase study of two- and three-dimensional porous tin(IV) selenides. *J. Mater. Chem.* **1999**, *9*, 1263–1274.
- (24) (a) Wang, C.; Bu, X.; Zheng, N.; Feng, P. Nanocluster with One Missing Core Atom: A Three-Dimensional Hybrid Superlattice Built from Dual-Sized Supertetrahedral Clusters. *J. Am. Chem. Soc.* **2002**, *124*, 10268–10269. (b) Su, W.; Huang, X.; Li, J.; Fu, H. Crystal of Semiconducting Quantum Dots Built Upon Covalently Bonded T5  $[\text{In}_{29}\text{Cd}_6\text{S}_{54}]^{-12}$ : The Largest Supertetrahedral Cluster in Solid State. *J. Am. Chem. Soc.* **2002**, *124*, 12944–12945.
- (25) Wang, C.; Li, Y.; Bu, X.; Zheng, N.; Zivkovic, O.; Yang, C.; Feng, P. Three-Dimensional Superlattices Built from  $(\text{M}_4\text{In}_{16}\text{S}_{33})^{10-}$  ( $\text{M} = \text{Mn}, \text{Co}, \text{Zn}, \text{Cd}$ ) Supertetrahedral Clusters. *J. Am. Chem. Soc.* **2001**, *123*, 11506–11507.
- (26) Brown, I. D. VALENCE: a program for calculating bond valences. *J. Appl. Crystallogr.* **1996**, *29*, 479–480.
- (27) Parise, J. B.; Ko, Y. Material Consisting of Two Interwoven 4-Connected Networks: Hydrothermal Synthesis and Structure of  $[\text{Sn}_5\text{S}_9\text{O}_2][\text{HN}(\text{CH}_3)_3]_2$ . *Chem. Mater.* **1994**, *6*, 718–720.
- (28) Zheng, N.; Bu, X.; Feng, P. Nonaqueous Synthesis and Selective Crystallization of Gallium Sulfide Clusters into Three-Dimensional Photoluminescent Superlattices. *J. Am. Chem. Soc.* **2003**, *125*, 1138–1139.
- (29) Yaghi, O. M.; Sun, Z.; Richardson, D. A.; Groy, T. L. Directed Transformation of Molecules to Solids: Synthesis of a Microporous Sulfide from Molecular Germanium Sulfide Cages. *J. Am. Chem. Soc.* **1994**, *116*, 807–808.
- (30) Zheng, N.; Bu, X.; Feng, P. Self-Assembly of Novel Dye Molecules and  $[\text{Cd}_8(\text{SPh})_{12}]^{4+}$  Cubic Clusters into Three-Dimensional Photoluminescent Superlattice. *J. Am. Chem. Soc.* **2002**, *124*, 9688–9689.
- (31) Cahill, C. L.; Parise, J. B. Synthesis and Structure of  $\text{MnGe}_4\text{S}_{10} \cdot (\text{C}_6\text{H}_{14}\text{N}_2) \cdot 3\text{H}_2\text{O}$ : A Novel Sulfide Framework Analogous to Zeolite Li-A(BW). *Chem. Mater.* **1997**, *9*, 807–811.
- (32) Bu, X.; Zheng, N.; Li, Y.; Feng, P. Templated Assembly of Sulfide Nanoclusters into Cubic- $\text{C}_3\text{N}_4$  Type Framework. *J. Am. Chem. Soc.* **2003**, *125*, 6024–6025.
- (33) Ahari, H.; Garcia, A.; Kirkby, S.; Ozin, G. A.; Young, D.; Lough, A. J. Self-assembling iron and manganese metal-germanium-selenide framework:  $[\text{NMe}_4]_2\text{MGe}_4\text{Se}_{10}$ , where  $\text{M} = \text{Fe}$  or  $\text{Mn}$ . *J. Chem. Soc., Dalton Trans.* **1998**, 2023–2027.
- (34) Pirani, A. M.; Mercier, P. A.; Dixon, D. A.; Borrmann, H.; Schrobilgen, G. J. Syntheses, Vibrational Spectra, and Theoretical Studies of the Adamantanoid  $\text{Sn}_4\text{Ch}_{10}^{4-}$  ( $\text{Ch} = \text{Se}, \text{Te}$ ) Anions: X-ray Crystal Structures of  $[\text{18-Crown-6-K}]_4[\text{Sn}_4\text{Se}_{10}] \cdot 5\text{en}$  and  $[\text{18-Crown-6-K}]_4[\text{Sn}_4\text{Te}_{10}] \cdot 3\text{en} \cdot 2\text{THF}$ . *Inorg. Chem.* **2001**, *40*, 4823–4829.
- (35) Krebs, B.; Voelker, D.; Stiller, K. Novel Adamantane-like Thio- and Selenoanions from Aqueous Solutions:  $\text{Ga}_4\text{S}_{10}^{8-}$ ,  $\text{In}_4\text{S}_{10}^{8-}$ ,  $\text{In}_4\text{Se}_{10}^{8-}$ . *Inorg. Chim. Acta* **1982**, *65*, L101–L102.
- (36) Palchik, O.; Iyer, R. G.; Liao, J. H.; Kanatzidis, M. G.  $\text{K}_{10}\text{M}_4\text{Sn}_4\text{S}_{17}$  ( $\text{M} = \text{Mn}, \text{Fe}, \text{Co}, \text{Zn}$ ): Soluble Quaternary Sulfides with the Discrete  $[\text{M}_4\text{Sn}_4\text{S}_{17}]^{10-}$  Supertetrahedral Clusters. *Inorg. Chem.* **2003**, *42*, 5052–5054.
- (37) Dehnen, S.; Brandmayer, M. K. Reactivity of Chalcogenostannate Compounds: Syntheses, Crystal Structures, and Electronic properties of Novel Compounds Containing Discrete Ternary Anions  $[\text{M}^{\text{II}}_4(\mu_4\text{-Se})(\text{SnSe}_4)_4]^{10-}$  ( $\text{M}^{\text{II}} = \text{Zn}, \text{Mn}$ ). *J. Am. Chem. Soc.* **2003**, *125*, 6618–6619.
- (38) Zimmermann, C.; Melullis, M.; Dehnen, S. Reactivity of Chalcogenostannate Salts: Unusual Synthesis and Structure of a compound Containing Ternary Cluster Anions  $[\text{Co}_4(\mu_4\text{-Se})(\text{SnSe}_4)_4]^{10-}$ . *Angew. Chem., Int. Ed.* **2002**, *41*, 4269–4272.
- (39) Eichhofer, A.; Fenske, D. Syntheses and structures of new copper(I)-indium(III)-selenide clusters. *J. Chem. Soc., Dalton Trans.* **2000**, 941–944.
- (40) Jin, X.; Tang, K.; Jia, S.; Tang, Y. Synthesis and Crystal Structure of a polymeric Complex  $[\text{S}_4\text{Cd}_{17}(\text{SPh})_{24}(\text{CH}_3\text{OCS}_2)_{4/2}]_n \cdot n\text{CH}_3\text{OH}$ . *Polyhedron* **1996**, *15*, 2617–2218.
- (41) Vossmeier, T.; Reck, G.; Schulz, B.; Katsikas, L.; Weller, H. Double-Layer Superlattice Structure Built Up of  $\text{Cd}_{32}\text{S}_{14}(\text{SCH}_2\text{CH}(\text{OH})\text{CH}_3)_{36} \cdot 4\text{H}_2\text{O}$  Clusters. *J. Am. Chem. Soc.* **1995**, *117*, 12881–12882.
- (42) Behrens, S.; Bettenhausen, M.; Deveson, A. C.; Eichhofer, A.; Fenske, D.; Lohde, A.; Woggon, U. Synthesis and Structure of the Nanoclusters  $[\text{Hg}_{32}\text{Se}_{14}(\text{SePh})_{36}]$ ,  $[\text{Cd}_{32}\text{Se}_{14}(\text{SePh})_{36}(\text{PPh})_4]$ ,  $[\text{P}(\text{Et})_2(\text{Ph})\text{C}_4\text{H}_8\text{OSiMe}_3]_5[\text{Cd}_{18}\text{I}_{17}(\text{PSiMe}_3)_{12}]$ , and  $[\text{N}(\text{Et})_3\text{C}_4\text{H}_8\text{OSiMe}_3]_5[\text{Cd}_{18}\text{I}_{17}(\text{PSiMe}_3)_{12}]$ . *Angew. Chem., Int. Ed. Engl.* **1996**, *35*, 2215–2218.

AR0401754